

The Influence of Surface Roughness and Cavitation on Journal Bearings: A Computational Study

Muhammad Sagaf

Department of Mechanical Engineering, Faculty of Engineering, Diponegoro University

Nazaruddin Sinaga

Department of Mechanical Engineering, Faculty of Engineering, Diponegoro University

Muhammad Tauviqirrahman

Department of Mechanical Engineering, Faculty of Engineering, Diponegoro University

Muhammad Khafidh

Department of Mechanical Engineering, Faculty of Industrial Technology, Universitas Islam Indonesia

他

<https://doi.org/10.5109/7388841>

出版情報 : Evergreen. 12 (3), pp.1458-1467, 2025-09. Interdisciplinary Graduate School of Engineering Sciences, Kyushu University, Japan

バージョン :

権利関係 : Creative Commons Attribution 4.0 International



The Influence of Surface Roughness and Cavitation on Journal Bearings: A Computational Study

Muhammad Sagaf^{1,3,*}, Nazaruddin Sinaga¹, Muhammad Tauviqirrahman¹,
Muhammad Khafidh², Althesa Androva^{1,4}, Akhmad Syakhroni^{1,3}

¹Department of Mechanical Engineering, Faculty of Engineering, Diponegoro University, Jl. Prof. Soedarto S.H. Tembalang, Semarang 50275, Indonesia

²Department of Mechanical Engineering, Faculty of Industrial Technology, Universitas Islam Indonesia, Jl. Kaliurang km 14.5, Sleman, Yogyakarta 55584, Indonesia

³Department of Industrial Engineering, Faculty of Industrial Technology, Universitas Islam Sultan Agung, Jl. Kaligawe Raya Km.4, Semarang 50111, Indonesia

⁴Department of Mechanical Engineering, Faculty of Engineering and Informatic, Universitas PGRI Semarang, Jl Sidodadi Timur No. 24, Semarang, 50125, Indonesia

*Author to whom correspondence should be addressed:
E-mail: msagaf@unissula.ac.id

(Received October 05, 2024; Revised July 29, 2025; Accepted August 31, 2025)

Abstract: The influence of surface roughness on journal bearings is interesting to study because of its influence on improving their performance. This study examines the influence of introducing surface roughness on the performance of bearings with the objective of improving lubrication, reducing cavitation, and minimizing noise. This research analyzes tribological features using a numerical approach in commercial CFD (computational fluid dynamics) software. Numerical results demonstrate that surface roughness improves bearing performance. These enhancements are notable in comparison to traditional journal bearings because they have a higher capacity to carry loads, a lower coefficient of friction, and produce less noise. On smooth journal bearings, the load carrying capacity, friction force, and average acoustic power level are 3171.34 N, 1123.6 N, and 80.6 dB, respectively. The roughness variation of Ra 12.5 on journal bearings results in 4650.5 N, 993.1 N, and 76.7 dB. Performance improved with a 46.6% increase in load capacity, an 11.6% reduction in friction, and a 4.8% decrease in noise, confirming the effectiveness of the proposed method.

Keywords: Cavitation; CFD; Journal Bearing; Surface roughness

1. Introduction

In the long run, the operation of the mechanical system is a fundamental concern, and the relative motion between two engine components has a significant impact on how well the system functions. Bearing systems are employed to offer support for the different mobile components of machines because of their notable simplicity and precision. Journal bearings are preferred in the industrial world, one of the reasons why they are advantageous is due to their ease of installation, minimal maintenance costs, and great damping capacity¹), low manufacturing costs, an easy manufacturing process, and a long service life²) can withstand heavy loads and high speeds in a stable and safe manner^{3,4}), even when used for high loading, speed, and precision in combustion motors, turbines⁵), compressors, and pumps⁶). Therefore, a variety of industrial machines

widely utilize sliding bearings as one of their key components. The shipbuilding industry, transportation equipment, pharmaceutical products, and food products are just a few examples⁷). Effective lubrication of journal bearings is essential in real-world applications. The lubricating system should be engineered to function with minimal energy consumption, optimal performance, and minimal noise throughout a range of loads, speeds, and conditions⁸). Typically, as temperature increases, the viscosity of lubricant decreases. Viscosity index enhancers, composed of oils containing highly polymeric molecules, are employed to reduce viscosity fluctuations during high-speed and heavy-load operations, particularly when temperatures rise. Augmenting the viscosity of the altered lubricant can improve its ability to support weight, even though viscosity typically diminishes with higher rates of deformation. Pseudoplasticity is the term that is used to

characterize this phenomenon. Zuraidah Rasep⁹⁾ conducted studies indicating that use RBD palm oil as a lubricant can enhance the performance of journal bearings. The effectiveness of journal bearings is contingent upon the presence of surface roughness, a factor that should not be disregarded. A number of scholars have examined the influence of surface roughness on bearing surfaces^{10,11)}. Gururajan and Prakash^{12,13)} conducted a study to examine how surface roughness affects the performance of lubricated short and long porous journal bearings. The results indicated a substantial correlation between the slide effect and the roughness. Naduvinamani et al.¹⁴⁾ conducted a study to examine the impact of surface roughness on porous journal bearings by employing coupled tension fluids. The researchers found that the bearing capabilities of coupled tension fluids were significantly impacted by surface roughness. Javorova¹⁵⁾ proposed that the impact of surface roughness should be considered in elastic conditions, where the film thickness value increases with increasing waviness amplitude, which corresponds to a reduction in hydrodynamics. Subsequently, Tauviqirrahman et al.¹⁶⁾ made the finding that surface roughness has the effect of decreasing both the hydrodynamic pressure and load-bearing capacity. It was assumed that the entire surface of the bushing was intentionally made rough in their case. The testing results demonstrated a significant correlation between the friction coefficient and the surface roughness¹⁷⁾. Furthermore, integrating the longitudinal roughness surface pattern¹⁸⁾ can improve the stability of the bearing. According to the numerical research, an elevation in surface roughness is linked to a decrease in pressure, load support, and deformation. Surface roughness can be artificially added to improve the performance of a journal bearing¹⁹⁾. The surface roughness produced for lubrication purposes is between 1 and 20 μm ²⁰⁾.

Meng and Zhang²¹⁾ conducted a study utilizing the Computational Fluid Dynamics (CFD) method to investigate the impact of compound groove texture on noise in sliding bearings. The research findings indicate that the compound groove texture significantly decreases the acoustic power level in the sliding bearing. Meng et al.²²⁾ conducted further research via experimental techniques with a tribotester and confirmed consistent findings, demonstrating that compound textures effectively reduce the average acoustic power level. Furthermore, the angular velocity of the shaft and the particular type of lubricant significantly affect the noise levels. Meng²³⁾ enhanced the research methods by taking into account the thermal impacts. The research findings indicate that the heat impact of the lubricant decreased the average acoustic level performance.

Furthermore, the presence of roughness has an impact on the occurrence of cavitation in sliding bearings²⁴⁾. The degree of surface roughness can significantly affect

cavitation, which in turn has substantial implications on load support and friction performance²⁵⁾. Cavitation greatly impacts the hydrodynamic performance of sliding bearings²⁶⁾. Hence, it is imperative to consider the impact of cavitation when assessing the effects of surface roughness on the bearing surface.

After conducting an extensive examination of relevant literature, it has been determined that the tribological behavior of a bearing is greatly impacted by the characteristics of its surface roughness. In addition, the experiments did not examine the noise and acoustic characteristics of journal bearings that were roughened and greased using lubrication fluids. The question of whether surface roughness in a journal bearing can simultaneously result in favorable tribological performance and reduced noise is a subject of ongoing discussion.

The primary aim of this work is to comprehensively analyze the lubricated bearings' tribological and acoustic properties, with particular focus on the influence of cavitation and roughness. To achieve more precise predictions of bearing performance, it is necessary to develop more complex computer models. This paper conducts a thorough analysis of journal bearings that have both smooth and rough lubricated surfaces. Additionally, our study includes consideration of multiphase cavitation and turbulence to accurately represent real-world scenarios.

2. Methodology

2.1. Theory

After more than a century of development, the equations of fluid mechanics can only be solved correctly under a limited range of flow circumstances. Although the existing solutions are very helpful in comprehending fluid dynamics, they are rarely immediately useful for engineering analysis or design. Historically, other techniques have been demanded of engineers²⁷⁻²⁹⁾. The utilization of equation simplifications is the most prevalent method. Typically, these calculations require empirical data and a combination of dimensional analysis and approximations³⁰⁾. Surface texture is a unique characteristic that is intentionally identified on a surface. Surface roughness, in contrast to texture, is frequently characterized by irregularity and can be difficult to identify³¹⁾.

2.1.1. Surface roughness modelling

Figure 1 illustrates the present study's modeling of the influence of an actual, rough surface on the movement of lubricant inside the bearing, employing a model that includes sand particles.

On this surface, there is a consistent layer of closely packed spheres, with each sphere having a specific diameter of K_s . The geometric surface roughness height, sometimes referred to as roughness height K_s , is distinct from the

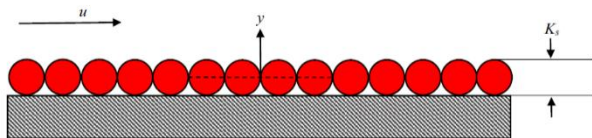


Fig. 1: Uniform sand-grain roughness model schematic

roughness height of sand particles that can be compared to it.

In order to calculate the sand particle roughness that is equivalent to the geometric roughness of the surface's height, a conversion factor must be utilized. The irregularity height K_s is denoted by the parameter R_a in this investigation. A profilometer is the actual instrument used to measure R_a , or the roughness pattern's arithmetic mean. The irregularity of the bearing will be determined by utilizing the value of R_a as the input for all calculations. The investigation conducted by Adams et al.³²⁾ demonstrated a clear relationship between K_s and R_a , which can be interpreted in the following manner:

$$K_s = 5.863R_a \tag{1}$$

2.1.2. Cavitation model

CFD software generates the mixed model of cavitation for this investigation. The mixture model demonstrates the flow of both vapor and liquid in a two-phase system. At the point where the pressure of the lubricant coating drops below the vaporization pressure, the transition phase from the liquid to the vapor takes place. The Eulerian model, a comprehensive multiphase model, was chosen due to its nearly comparable performance compared to the mixture model. This decision was based on the reduced computational cost of the Eulerian model³³⁾. Furthermore, the bearing has shown that the mixing model is suitable for managing vapor-phase volume fractions of significant size. This method is also employed to measure the expansion of gas bubbles that commonly occur during the cavitation phenomenon. The Zwart-Gelber-Belamri³⁴⁾ multiphase cavitation model is specifically employed in this study. The vapor transfer equation is a mathematical expression that represents the transmission of mass between the phase of liquid and vapor during the evaporation, and condensation process that takes place within cavitation.

$$\frac{\partial}{\partial t}(\alpha_v \rho_v) + \nabla \cdot (\alpha_v \rho_v V) = R_g - R_c \tag{2}$$

The symbol α_v represents the fraction of volume occupied by vapor, whereas ρ_v represents the density of the vapor. The process of exchanging mass between the liquid and vapor phases during cavitation is facilitated by R_g and R_c . The ultimate expression of cavitation in the^{34,35)} model is depicted as follows, assuming that each bubble in a system has the same size:

$$p \leq p_v, R_g = F_{evap} \frac{3\alpha_{nuc}(1-\alpha_v)\rho_v}{R_{bl}} \sqrt{\frac{2}{3}} \frac{p_v - p}{\rho} \tag{3}$$

$$p \leq p_v, R_c = F_{cond} \frac{3\alpha_v \rho_v}{R_{bl}} \sqrt{\frac{2}{3}} \frac{p - p_v}{\rho} \tag{4}$$

The variables in the equation are as follows: p_v represents the vapor pressure, ρ represents the liquid density, α_{nuc} represents the nucleation site volume percentage which is equal to 5×10^{-4} , and R_{bl} represents the bubble radius which is $10^{-6}m$. The evaporation coefficient, F_{evap} , has a value of 50, whereas the condensation coefficient, F_{cond} , has a value of 0.01. All values given here are obtained from published sources^{34,35)}.

The Zwart-Gelber-Belamri multiphase cavitation model has been used for journal speeds ranging from 1000 to 4000 rpm and eccentricity ratios from 0.1 to 0.9³⁶⁻³⁸⁾. It is effective in simulating cavitation under high rotational speeds and varying eccentricity ratios, which are common in industrial applications^{36,39)}. The model has been applied to bearings lubricated with different types of oils, including nano-lubricants with various nanoparticle volume fractions, demonstrating its versatility in different lubrication scenarios^{37,38)}. The model has been validated under different load conditions, showing significant impacts on pressure distribution, cavity volume, and load-bearing capacity^{38,39)}. It is particularly useful in predicting the performance of bearings under high load and high-speed conditions, where cavitation is more likely to occur^{36,39)}. The Zwart-Gerber-Belamri model has been validated against experimental and numerical data, with deviations not exceeding 3%, indicating high accuracy and reliability in predicting cavitation phenomena^{36,37,39)}.

2.2. Geometry

The journal bearing, which has a rotating shaft in relation to the housing, is shown in Figure 2. The gap that exists between the two sides of the journal bearing is filled with lubricant in order to prevent any deficiencies in lubrication from transpiring.

The lubricating fluid layer thickness between the two surfaces can be calculated using Equation 5.

$$h(\theta) = c(1 + \varepsilon \cos \theta) \tag{5}$$

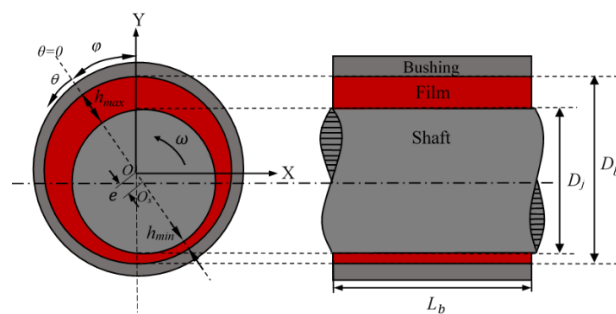


Fig. 2: Journal bearing schema

Table 1: Journal Bearing Parameter

Journal bearing parameter	Symbol	Value	Unit
Bearing			
Journal diameter	D_j	50	mm
Bushing diameter	D_b	50.1	mm
Bushing length	L_b	25	mm
Radial clearance	c	0.05	mm
Eksentrisitas ratio	ϵ	0.8	-
Attitude Angle	ϕ	30°	-
Shaft rotational speed	ω	4000	rpm
Oil			
Oil liquid density	ρ_f	850	kg/m ³
Oil liquid viscosity	μ_o	0.0125	Pa.s
Oil vapour density	ρ_v	10.95	kg/m ³
Oil vapour viscosity	μ_v	2×10^{-5}	Pa.s
Saturated pressure vapour	P_{sat}	29,185	Pa

Define $h(\theta)$ as the fluid's vertical distance at an angle θ . The radial clearance, or the numerical difference between the radius of the shaft and the radius of the housing, is represented by the variable c . The relationship between eccentricity and radial clearance is represented by the symbol ϵ . A journal bearing is a specialized form of bearing that provides support to a spinning shaft by utilizing a thin layer of lubrication between the shaft and the bearing surface. The research employs Dhande's unique journal-bearing geometry³³⁾ to simulate various fluid flow situations. According to the information provided in Table 1, this shape utilizes the unique properties of the journal bearing and the lubricating fluid.

2.3. Meshing

This simulation only requires meshing for fluid geometry in Fluent, ignoring structural geometries. Table 2 contains both meshing data and meshing output. In the axial, circumferential, and radial orientations, the mesh output is $50 \times 356 \times 6$.

2.4. Material Definition and Boundary Conditions

The configuration employs the Zwart-Gerber-Belamri cavitation model, laminar flow, mixture mode, and liquid

Table 2: Meshing Fluid Domain Newtonian Criteria

Mesh criteria	Number
Face sizing	6-layers of division
Method	Multizone
Element number	149688
Node number	177408
Maximum skewness	0.99997
Minimum skewness	2.3367×10^{-2}
Average skewness	0.8018

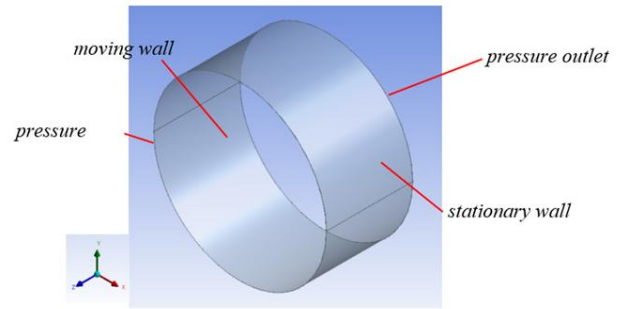


Fig. 3: Definition of lubricating fluids

and vapor phases in two-phase modeling. Figure 3 illustrates the material definition for lubricating fluids. Figure 4 depicts the pressure inlet and exhaust as the boundary conditions in this simulation. The moving wall's speed is 4000 rpm, and the pressure value on the entrance and exit sides is 0.

This work employs fluid flow modeling to analyze incompressible fluid flows occurring at low fluid rates. We utilize a pressure-based solver including the SIMPLE method to conduct all of the case simulations.

The configuration of the spatial discretization for gradients, pressure, momentum, volume fraction, turbulent kinetic energy, turbulent dissipation rate, and transient formulation in this final task should be done in accordance with the parameters that are mentioned in Table 3. In comparison to alternative discretization approaches, this specific configuration produces simulation outcomes that are both rapid and precise.

In order to enhance the precision of fluid flow simulation outcomes, it is essential to determine the convergence

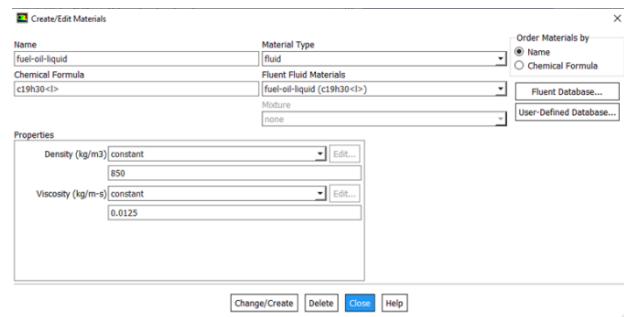


Fig. 4: Fluid domain boundary conditions

Table 3: Simulation Method

Simulation Method	Simulation Method Type
Scheme	SIMPLE
Gradient	Least Squares Cell Based
Pressure	PRESTO!
Momentum	Second Order Upwind
Volume Fraction	QUICK
Turbulent Kinetic Energy	Second Order Upwind
Turbulent Dissipation Rate	Second Order Upwind

threshold for the iteration process. The convergence threshold is set to 10^{-4} .

3. Result

An application of the Computational Fluid Dynamics (CFD) methodology was applied in order to carry out a simulation in this particular situation. The objective of this study is to analyze the effects on the performance of journal bearings, including factors such as load-carrying capacity, acoustic power level, and friction force. A simulation was performed to evaluate the performance of journal bearings with both smooth and rough surfaces for the purpose of comparison. The angular speed used was 4000 rpm with an eccentricity ratio of $\epsilon = 0.8$.

3.1. Validation

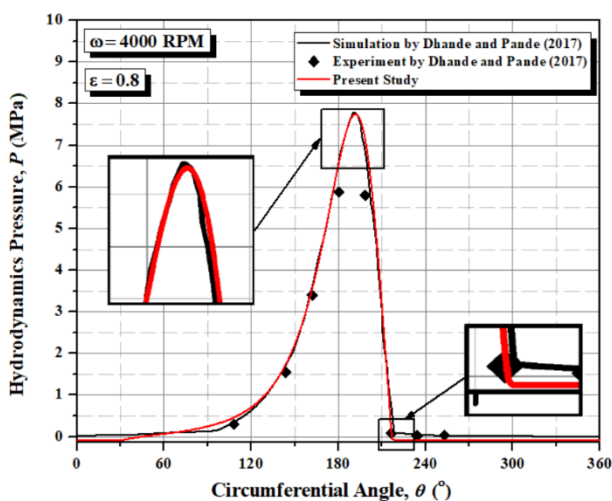


Fig. 5: Validation result of hydrodynamic pressure distribution³³⁾

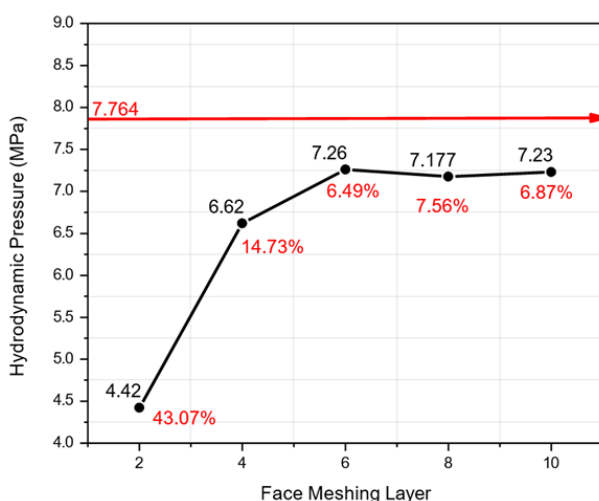


Fig. 6: Grid independence of journal bearing with $\epsilon = 0.8$ and $\omega = 4000$ rpm

Table 4: Comparison of Maximum Pressure Value of Journal Bearing at $\epsilon = 0.8$, $\omega=4000$ rpm Between Dhande and Pande's Simulation³³⁾ and Present Study Simulation

Objectives	Unit	Dhande and Pande	Present Study	Error (%)
Maximum Hydrodynamic Pressure, P_{max}	Mpa	7.764	7.26	6.49
Maximum Bearing Deformation, S_{max}	μm	0.647	0.644	0.46

To ensure acceptance, the numerical methodology and its solution configuration in commercial CFD must yield accurate results that meet the specified accuracy. This can be achieved by validating the results against those of previous published studies. This study validated the hydrodynamic pressure distribution of Dhande and pande³³⁾ using numerical data and experimental results. Calculations were carried out using identical input conditions and operational parameters as references. Figure 5 displays the results of this study validation. Validation on the current numerical method was selected at a rotation speed of 4000 rpm, producing a maximum hydrodynamic value 6 percent lower than the value in the Dhande and Pande³³⁾ study, which was 7.26 Mpa, as shown in Table 4. It can be concluded that the results of the current study are in accordance with the results of the Dhande and Pande³³⁾ study used as a reference. This shows that the established numerical solution code has been validated. Furthermore, all simulations are based on the existing code.

Figure 6 displays the outcomes of the grid independence test performed for the simulation at an eccentricity of 0.8 and a rotational speed of 4000 RPM. The test entailed enhancing the mesh by augmenting the quantity of facial layers. The results demonstrated reliable outcomes, and in light of the necessity for decreased processing time, six face layers were identified as the ideal arrangement. This mesh arrangement was thereafter established as the standard for all subsequent simulations.

3.2. Smooth journal bearing

A journal bearing with a smooth surface roughness level is depicted in Figures 7, 8, and 9.

3.3. Rough journal bearing

Figure depicts the schematic representation of a partially roughened journal bearing with a geometric shape. Figure 10 and 11 displays the profile of the surface roughness area. Figures 12, 13, and 14 depict the variations in static pressure, volume fraction, and acoustic power level for a journal bearing with an eccentricity ratio (ϵ) of 0.8, operating under conditions of rough surface roughness with a R_a value of 12.5.

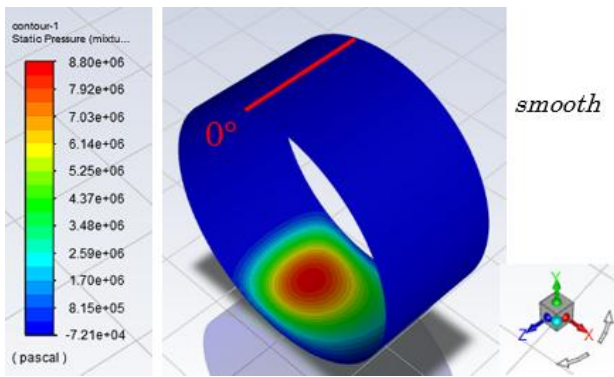


Fig. 7: Pressure distribution contours in smooth journal bearings

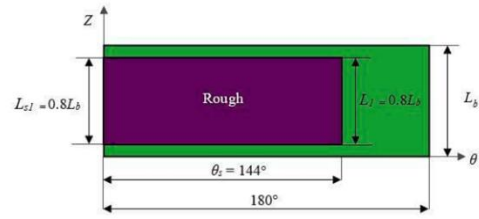


Fig. 11: Surface roughness area profile

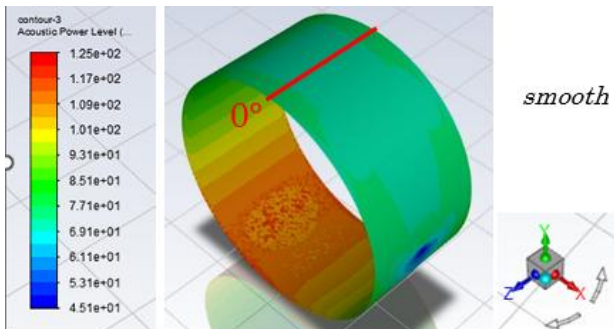


Fig. 8: Acoustic Power Level Contour in smooth journal bearings

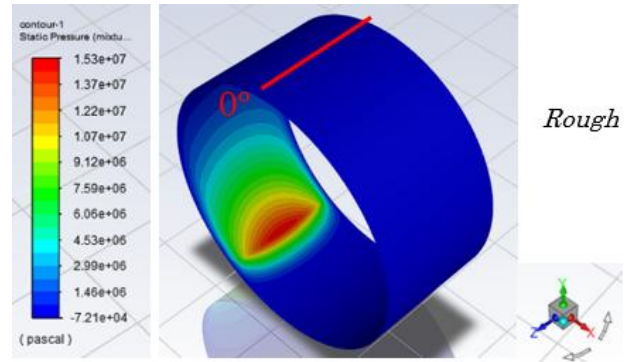


Fig. 12: Pressure distribution contours in rough journal bearings (Ra=12.5)

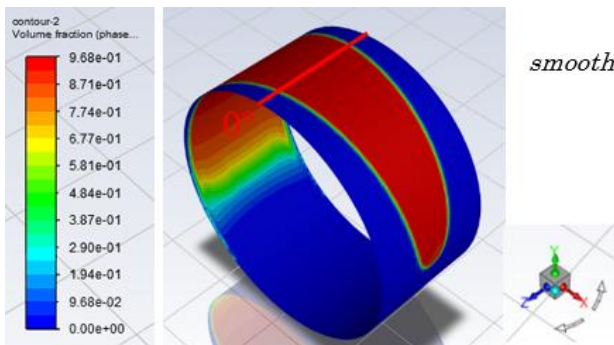


Fig. 9: Volume fraction contour in smooth journal bearings

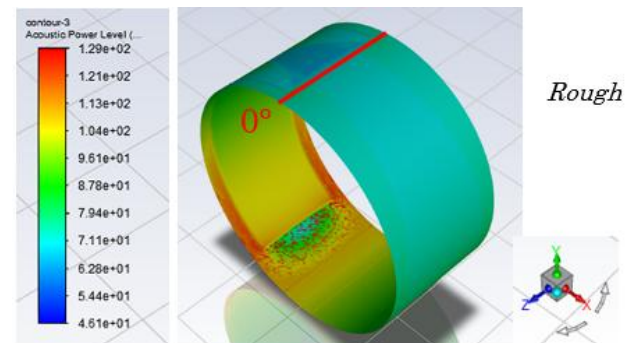


Fig. 13: Acoustic power level contours in rough journal bearings (Ra=12.5)

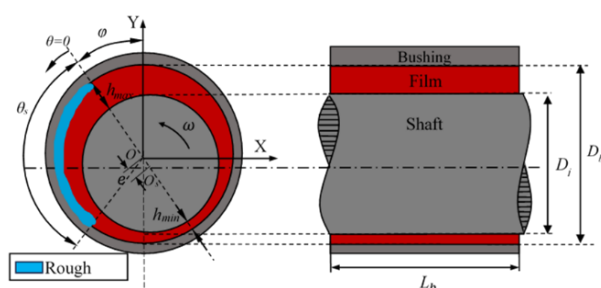


Fig. 10: Geometri partial rough journal bearing scheme

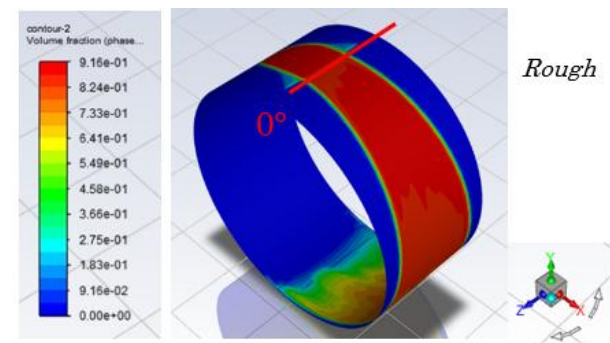


Fig. 14: Volume fraction contours in rough journal bearings (Ra=12.5)

3.4. Effect of surface roughness

Figure 15 displays the outcomes of simulations conducted in lubricated journal bearing, indicating that the highest pressure occurs within the angular range of 160°–270° for smooth surfaces and 25°–200° for rough surfaces. The

maximum pressures occur at a hardness level of $Ra = 12.5$. Figure 16 illustrates a comparison of the volume fractions of the two specimens. The graph demonstrates that cavitation processes initiate on smooth surfaces throughout the angle range of 0° – 165° and 260° – 360° . Cavitation occurs on rough surfaces within a specific range of angles 0° – 25° and 200° – 360° . The findings indicate that cavitation is accelerated on rough surfaces as a result of the heightened turbulence they generate in comparison to smooth surfaces. This phenomenon arises due to the fact that rough surfaces generate more pronounced and quick alterations in pressure on the surface, hence impacting the creation of steam bubbles.

Figure 17 displays the acoustic power level of the four specimens. Based on the graph shown, it is evident that rough surfaces produce higher peak noise levels in comparison to smooth surfaces. Upon closer examination, it becomes evident that surface roughness has the ability to reduce the average noise level in comparison to the smooth surface of the journal bearing. The decrease in acoustic power level can be attributed to the hindered creation of

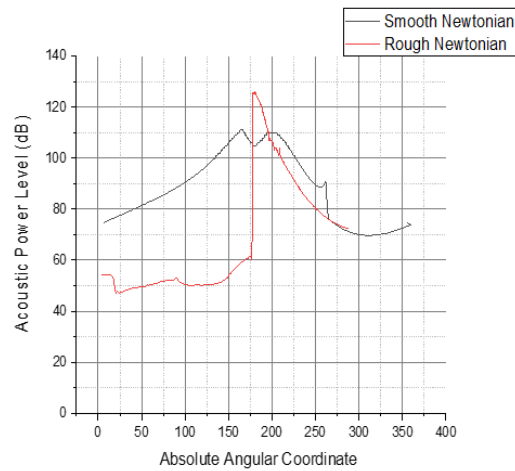


Fig. 17: Acoustic power level distribution of journal bearing with $\epsilon = 0.8$

turbulent lubricant flow caused by a significant roughness on the surface, which can be explained by the lubrication speed.

The results of a comparative investigation of the distribution of turbulent kinetic energy among the four specimens are presented in Figure 18. The preceding graph demonstrates the correlation between kinetic energy and eddy dissipation rate, illustrating that a decrease in the eddy dissipation rate results in a reduction in turbulent kinetic energy. This behavior is ascribed to a shared component, which can either diminish the turbulent movement of lubricant or impede turbulence from occurring on rough surfaces.

Figure 19 illustrates the dispersion of turbulent eddy dissipation over the four specimens. The graph demonstrates that the turbulent dissipation rate is lower on the rough surface as opposed to the smooth surface. This is attributed to the surface roughness value, which results in a reduced turbulent flow of lubricant or makes it more challenging to induce turbulence.

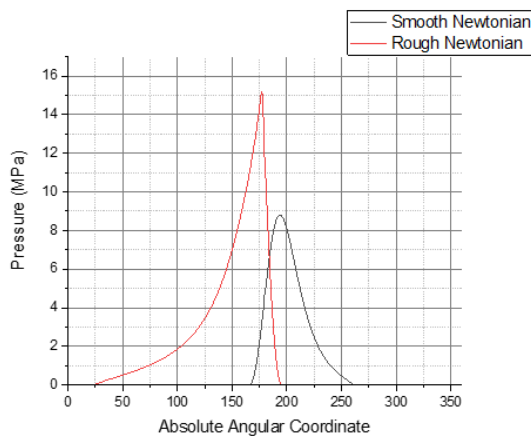


Fig. 15: Pressure distribution of journal bearing with $\epsilon = 0.8$

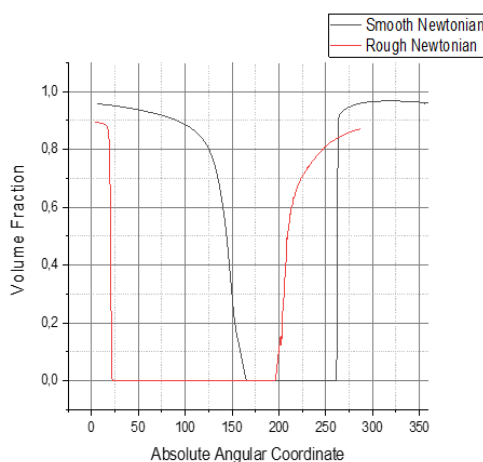


Fig. 16: Volume fraction distribution of journal bearing with $\epsilon = 0.8$

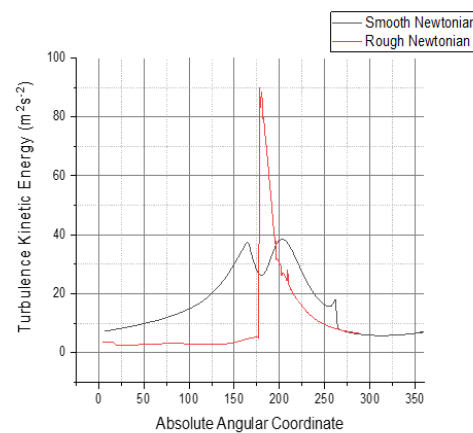


Fig. 18: Turbulent kinetic energy distribution of journal bearing with $\epsilon = 0.8$

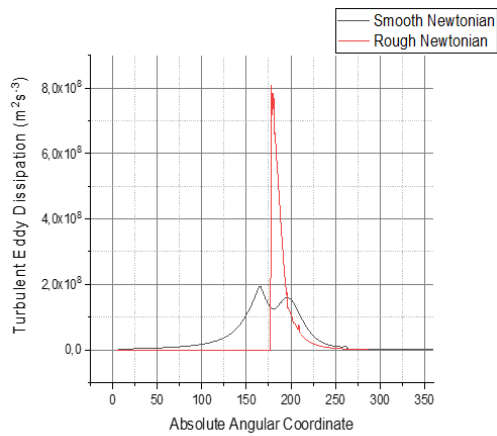


Fig. 19: Turbulent eddy dissipation distribution of journal bearing with $\epsilon = 0.8$

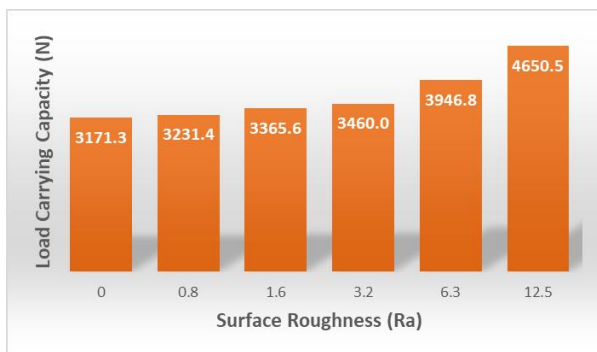


Fig. 20: Effect of surface roughness on load-carrying capacity of journal bearing with $\epsilon = 0.8$

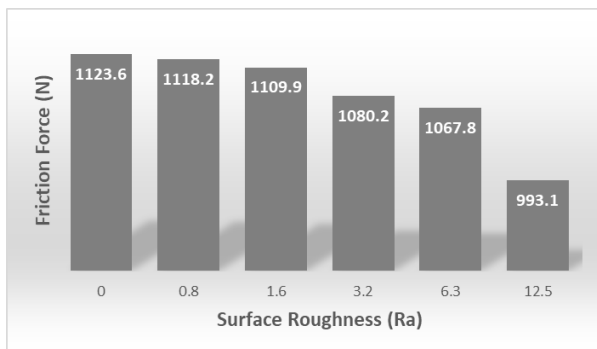


Fig. 21: Effect of surface roughness on friction force of journal bearing with $\epsilon = 0.8$

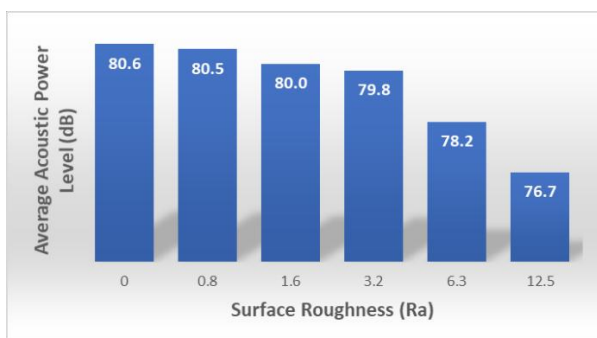


Fig. 22: Effect of surface roughness on average acoustic power level of journal bearing with $\epsilon = 0.8$

Figure 20 exhibits a direct association between the roughness parameter's magnitude and the load-carrying capacity value in convergent regions. The presence of surface irregularities in the convergent region leads to the elevation of pressure levels. This phenomenon is also known as the fluid hydrodynamic effect. Furthermore, the enhanced ability of the load-carrying capacity can be attributed to the capability of bearings that can withstand surface roughness in the area of convergence to more effectively absorb external loads and reduce shear stress in the lubricant caused by sudden changes in film thickness. Figure 21 shows the presence of surface roughness can lead to varying degrees of friction, which in turn impacts the performance of bearings. Decreasing the roughness is advantageous as it minimizes the amount of wear on the bearings. This phenomenon occurs due to the distortion of the asperity section, resulting in an augmentation of the fluid film's thickness and a reduction in the contact area with the shaft.

The average acoustic power output decreases as surface roughness rises as shown in Figure 22. The reduction in acoustic power level is attributed to the presence of roughness, as it affects the speed of lubricant distribution. A surface with high roughness value makes it more challenging for turbulent lubricant flow to experience turbulence, thereby impacting the acoustic value.

4. Conclusion

The findings of the research give rise to multiple inferences, which include the following:

The simulation findings produced using the surface roughness ratio have a considerable impact on the tribological and acoustic power level performance of journal bearings. Surface roughness enhances the distribution of pressure and the ability to bear loads, while simultaneously reducing friction force. When surface roughness is present, the average acoustic power level decreases, leading to a reduction in noise relative to when there is no surface roughness.

The analytical findings demonstrated an augmentation in the load-carrying capability, accompanied by a reduction in both the frictional force and the average acoustic power level within the journal bearing. This was observed for lubricated journal bearing, with a roughness variation of $Ra = 12.5$ and an eccentricity ratio of 0.8. The lubricated journal bearing produced load carrying capacity values of 4650.5 N, friction force of 993.1 N, and an average acoustic power level of 76.7 dB.

The results can guide the design of journal bearings in gas turbines, compressors, and hydraulic pumps, where cavitation and surface wear significantly impact efficiency and lifespan. The study's cavitation model can improve bearing durability in internal combustion engines and ship propulsion systems, where oil-film breakdown leads to

pitting and erosion. Wind turbine gearboxes and hydroelectric generators often suffer from bearing failures due to mixed lubrication regimes.

Acknowledgement

The research was funded by Sultan Agung Islamic University (UNISSULA).

References

- 1) D.Y. Dhande, and D.W. Pande, "Numerical Analysis of Multiphase Flow in Hydrodynamic Journal Bearing Using CFD Coupled Fluid Structure Interaction with Cavitation," in: *Int. Conf. Autom. Control Dyn. Optim. Tech.*, 2016: pp. 964–971. doi:10.1016/j.jksues.2016.09.001.
- 2) D. Benasciutti, M. Gallina, M.G. Munteanu, and F. Flumian, "A numerical approach for the analysis of deformable journal bearings," *Frat. Ed Integrita Strutt.*, 21 37–45 (2012). doi:10.3221/IGF-ESIS.21.05.
- 3) Y. Chen, Y. Sun, Q. He, and J. Feng, "Elastohydrodynamic behavior analysis of journal bearing using fluid–structure interaction considering cavitation," *Arab. J. Sci. Eng.*, 44 (2) 1305–1320 (2019). doi:10.1007/s13369-018-3467-9.
- 4) H. Chen, and Y. Zhang, "Hydrodynamic journal bearing with slippage sleeve surface," *Aust. J. Mech. Eng.*, 19 (2) 143–152 (2021). doi:10.1080/14484846.2019.1587812.
- 5) D.A. Bompos, and P.G. Nikolakopoulos, "Tribological design of a multistep journal bearing," *Simul. Model. Pract. Theory*, 68 18–32 (2016). doi:10.1016/j.simpat.2016.07.002.
- 6) S.B. Kalakada, P.N. Kumarapillai, and R.K. Perikinalil, "Analysis of static and dynamic performance characteristics of thd journal bearing operating under lubricants containing nanoparticles," *Int. J. Precis. Eng. Manuf.*, 13 (10) 1869–1876 (2012). doi:10.1007/s12541-012-0245-6.
- 7) E.N. Santos, C.J.C. Blanco, E.N. MacÊdo, C.E.A. Maneschy, and J.N.N. Quaresma, "Integral transform solutions for the analysis of hydrodynamic lubrication of journal bearings," *Tribol. Int.*, 52 161–169 (2012). doi:10.1016/j.triboint.2012.03.016.
- 8) N. Marey, E. Hegazy, H. El-gamal, A. Ali, and A. Bassam, "Journal bearing performance – state of the art," *Sylwan*, 165 (4) 390–416 (2021).
- 9) Z. Rasep, M. Noor, A. Witri, M. Yazid, S. Samion, N. Azwadi, and C. Sidik, "Numerical investigation into trapezoid surface texture of journal bearing and rbd palm oil as lubricant," *Evergreen*, 11 (02) 1389–1398 (2024). <https://doi.org/10.5109/7183451>
- 10) A. Bhattacharya, J.K. Dutt, and R.K. Pandey, "Influence of hydrodynamic journal bearings with multiple slip zones on rotordynamic behavior," *J. Tribol.*, 139 (6) (2017). doi:10.1115/1.4036629.
- 11) S. Cupillard, S. Glavatskih, and M.J. Cervantes, "Computational fluid dynamics analysis of a journal bearing with surface texturing," *Proc. Inst. Mech. Eng. Part J J. Eng. Tribol.*, 222 (2) 97–107 (2008). doi:10.1243/13506501JET319.
- 12) K. Gururajan, and J. Prakash, "Surface roughness effects in infinitely long porous journal bearings," *J. Tribol.*, 121 (1) 139–147 (1999). doi:10.1115/1.2833795.
- 13) K. Gururajan, and J. Prakash, "Effect of surface roughness in a narrow porous journal bearing," *J. Tribol.*, 122 (2) 472–475 (1999). doi:10.1115/1.555387.
- 14) N.B. Naduvinamani, P.S. Hiremath, and G. Gurubasavaraj, "Surface roughness effects in a short porous journal bearing with a couple stress fluid," *Fluid Dyn. Res.*, 31 (5–6) 333 (2002). doi:10.1016/S0169-5983(02)00137-5.
- 15) J. Javorova, "Ehd lubrication of journal bearings with rough surfaces," *Proceeding of the Intern. Conf.*, 2010 *Mech. Eng. XXI Century*, 1 149–152 (2010).
- 16) M. Tauviiqirrahman, B.C. Ichsan, Jamari, and Muchammad, "Influence of roughness on the behavior of three-dimensional journal bearing based on fluid-structure interaction approach," *J. Mech. Sci. Technol.*, 33 (10) 4783–4790 (2019). doi:10.1007/s12206-019-0919-4.
- 17) Q. Wen, M. Liu, Z. Zhang, and Y. Sun, "Experimental investigation into the friction coefficient of ball-on-disc in dry sliding contact considering the effects of surface roughness, low rotation speed, and light normal load," *Lubricants*, 10 (10) (2022). doi:10.3390/lubricants10100256.
- 18) A.K. Tomar, and S.C. Sharma, "Study on surface roughness and piezo-viscous shear thinning lubricant effects on the performance of hole-entry hybrid spherical journal bearing," *Tribol. Int.*, 168 107349 (2022). doi:<https://doi.org/10.1016/j.triboint.2021.107349>.
- 19) M. Sagaf, N. Sinaga, M. Tauviiqirrahman, M. Khafidh, and A. Androva, "Analysis of the journal bearing performance considering artificial surface roughness and cavitation using cfd fsi method," *AIP Conf. Proc.*, 2706 (May 2008) (2023). doi:10.1063/5.0120464.
- 20) A.A. Elsharkawy, "Surface roughness effect on finite journal bearings with flexible porous liners," *Lubr. Sci.*, 17 (4) 361–387 (2005). doi:10.1002/lvs.3010170402.
- 21) F.M. Meng, and W. Zhang, "Effects of compound groove texture on noise of journal bearing," *J. Tribol.*, 140 (3) 1–12 (2018). doi:10.1115/1.4038353.
- 22) F. Meng, H. Yu, C. Gui, and L. Chen, "Experimental

- study of compound texture effect on acoustic performance for lubricated textured surfaces,” *Tribol. Int.*, 133 (November 2018) 47–54 (2019). doi:10.1016/j.triboint.2018.12.036.
- 23) F. Meng, R. Shu, and L. Chen, “Influences of operation parameters on noise of journal bearing with compound texture considering lubricant thermal effect,” *Proc. Inst. Mech. Eng. Part J J. Eng. Tribol.*, 234 (7) 991–1006 (2020). doi:10.1177/1350650119868910.
 - 24) Z.P. He, J.H. Zhang, Z.Y. Li, L. Ba, G.C. Zhang, K.N. Wang, and X. Lu, “Inter-asperity cavitation for misalignment journal lubrication problem based on mass-conservative algorithm,” *J. Zhejiang Univ. Sci. A*, 14 (9) 642–656 (2013). doi:10.1631/jzus.A1300080.
 - 25) A. Czaban, “Cfd analysis of hydrodynamic lubrication of slide conical bearing with consideration of the bearing shaft and sleeve surface roughness,” *J. KONES. Powertrain Transp.*, 21 (3) 35–40 (2014). doi:10.5604/12314005.1133159.
 - 26) N. Sinaga, M. Tauviqirrahman, A.R. Hakim, and E. Yohana, “Effect of texture depth on the hydrodynamic performance of lubricated contact considering cavitation,” *IOP Conf. Ser. Mater. Sci. Eng.*, 494 (1) (2019). doi:10.1088/1757-899X/494/1/012047.
 - 27) A. Androva, M. Tuviqirrahman, N. Sinaga, M. Khafidh, and M. Sagaf, “Analysis of hydrophobic coating on load carrying capacity of journal bearing considering turbulence effect using cfd fsi method,” *AIP Conf. Proc.*, 2706 (May 2008) 8–13 (2023). doi:10.1063/5.0120603.
 - 28) A. Androva, M. Tauviqirrahman, N. Sinaga, M. Khafidh, M. Sagaf, and Hafid, “A comparative study on hydrodynamic analysis with and without cavitation modelling: a study on textured slip journal bearing,” *CFD Lett.*, 16 (8) 48–63 (2024). doi:10.37934/cfdl.16.8.4863.
 - 29) M. Sagaf, N. Sinaga, M. Tauviqirrahman, M. Khafidh, and A. Androva, “Effects of artificial roughness on journal bearings using non-newtonian lubricants: a cfd cavitation study,” *J. Adv. Res. Fluid Mech. Therm. Sci.*, 130 (1) 136–147 (2025). doi:10.37934/arfmts.130.1.136147.
 - 30) J.H.F. and M.Peric, “Computational Methods for Fluid Dynamics,” Fourth, Rev.Stanford:Springer, 2020. <https://link.springer.com/book/10.1007/978-3-319-99693-6>
 - 31) D. Gropper, L. Wang, and T.J. Harvey, “Hydrodynamic lubrication of textured surfaces: a review of modeling techniques and key findings,” *Tribol. Int.*, 94 509–529 (2016). doi:10.1016/j.triboint.2015.10.009.
 - 32) T. Adams, C. Grant, and H. Watson, “A simple algorithm to relate measured surface roughness to equivalent sand-grain roughness,” *Int. J. Mech. Eng. Mechatronics*, 1 (1) (2012). doi:10.11159/ijmem.2012.008.
 - 33) D.Y. Dhande, and D.W. Pande, “A two-way fsi analysis of multiphase flow in hydrodynamic journal bearing with cavitation,” *J. Brazilian Soc. Mech. Sci. Eng.*, 39 (9) 3399–3412 (2017). doi:10.1007/s40430-017-0750-8.
 - 34) P.J. Zwart, A.G. Gerber, and T. Belamri, “A two-phase flow model for predicting cavitation dynamics,” *5th Int. Conf. Multiph. Flow*, 152 (January 2004) 152 (2004).
 - 35) T.D. Canonsburg, “ANSYS fluent tutorial guide,” 15317 (November) 724–746 (2013).
 - 36) Z.H. Kadhim, L. Hammed, F.A. Rahima, and A.M. Ridha, “Elastohydrodynamic analysis of a journal bearing with different grade oils considering thermal and cavitation effects using cfd-fsi,” *Diagnostyka*, 24 (2) 1–10 (2023). doi:10.29354/diag/166102.
 - 37) B.A. Abass, S.Y. Ahmed, and Z.H. Kadhim, “Analysis and optimization of nanolubricated journal bearing under thermoelasto-hydrodynamic lubrication considering cavitation effect,” *Tribol. Ind.*, 45 (4) 618–633 (2023). doi:10.24874/ti.1441.01.23.04.
 - 38) B.A. Abass, S.Y. Ahmed, and Z.H. Kadhim, “Thermoelasto-hydrodynamic analysis of nanolubricated journal bearings using computational fluid dynamics with two-way fluid–structure interaction considering cavitation,” *Arab. J. Sci. Eng.*, 48 (3) 2939–2950 (2023). doi:10.1007/s13369-022-07024-9.
 - 39) Y. Taghipour, P. Akbarzadeh, F. Moradgholi, and M. Eftekhari Yazdi, “Numerical study of the cavitation effect on plain bearings in constant and variable viscosity states,” *Meccanica*, 56 (10) 2507–2516 (2021). doi:10.1007/s11012-021-01391-7.